Characterization of an End Product in a Copper(II)-Mediated Nonenzymatic Reaction of Vitamin B_6 with Amino Acid: X-Ray Crystal Structure of a Dimer of Cu(II)·[Pyridoxal 5-Phosphate–Pyridoxamine 5-Phosphate Schiff Base]·$7H_2O$

Toshimasa Ishida,* Yasuko In, Chiuru Hayashi, Reijiro Manabe, and Akio Wakahara*,†

Department of Physical Chemistry, Osaka University of Pharmaceutical Sciences, 4-20-1 Nasahara, Takatsuki, Osaka 569-11

†Fujisawa Pharmaceutical Co., Ltd., 2-1-6 Kashima, Yodogawa-ku, Osaka 532

(Received January 9, 1997)

A copper(II) complex of the Schiff base condensation of pyridoxal 5-phosphate (PLP) with pyridoxamine 5-phosphate (PMP) was precipitated as an end product during a nonenzymatic copper(II)-mediated transamination reaction of L-amino acid (alanine, leucine, lysine, glutamic acid, or glutamine) via Schiff base formation with PLP at pH = 2.5. The complex was determined by an X-ray crystal structure analysis to consist of a dimer of Cu(II)·[PLP–PMP Schiff base]·$7H_2O$, where a covalent bond is formed between the carbon atoms of neighboring Schiff base –C=N– fragments. The crystal consists of a racemate of the (*R*,*R*)- and (*S*,*S*)-configuration at the covalently bonded carbon atoms. By this bond formation and the phosphate O–Cu(II) coordination between neighboring dimers, complexes exist as a polymerized form in the crystal. The copper(II) ion forms a thermally stable square-pyramidal five-coordination with an azomethine nitrogen, two pyridine oxygens, a water oxygen, and a phosphate oxygen. Possible in vitro copper(II)-mediated formation of the complex from PLP and L-amino acid is considered.

In addition to the coenzyme of a number of enzymes which catalyze different types of reactions in amino acid metabolism,[1,2] pyridoxal 5-phosphate (PLP) plays various physiological functions as vitamin B_6. PLP itself, activated by a metal ion, is also known to catalyze various transformations of amino acid in a nonenzymatic model system.[3—5] This biomimetic reaction involves the formation of a Schiff base intermediate through condensation of the PLP carbonyl group and amino acid α-amino group.

Since it is believed that the reaction pathway of an amino acid (such as decarboxylation, transamination or racemization) is highly related to the stereochemical aspects of its Schiff base and each metabolite,[6] conformational studies have been carried out using various types of Schiff base derivatives.[7,8] In our continuation of an X-ray conformational study[9] of metal-complexed vitamin B_6–amino acid Schiff bases, this paper deals with the structural characterization of a copper(II) complex of the Schiff base condensation of PLP with pyridoxamine 5-phosphate (PMP), studied by spectroscopic and X-ray diffraction methods. The present complex crystal, which was precipitated as an end product during a Cu(II)-mediated transamination experiment of L-amino acids of alanine, leucine, lysine, glutamic acid, or glutamine via Schiff base formation with PLP under acidic conditions, was shown to consist of a dimer structure (**2**) of the Cu(II)·[PLP–PMP Schiff base] monomer (**1**).

Results and Discussion

Molecular Structure. The chemical structure of complex **2** is shown in Fig. 1. The molecular conformation of **2** and its interaction with the neighboring complex is shown in Fig. 2. Some selected bond lengths and angles, as well as the coordination parameters around the copper ion, are given in Tables 1 and 2, respectively. Because of the small crystal size and limited observable intensities, the bond lengths and angles[10] were not as accurate as usual. However, these factors would not significantly affect the structural description of the complex.

The present complex takes the dimerized structure (**2**) of the Cu(II)·[PLP–PMP Schiff base] monomer (**1**), where the bond lengths and angles around the covalently bonded C(4′) and c(14′) atoms are in the range of the usual sp^3-covalent bond, although the C(4′)–c(14′) bond length (1.62(2) Å) is somewhat longer than the generally accepted value (1.542 Å)[11] for the $(C\#)_2$–CH–CH–$(C\#)_2$ bond sequence, where C# indicates any C_{sp^3} atom. Judging from the bond lengths and angles, the electronic structure of the complex could be in the state of phosphate oxygen deprotonated, pyridine nitrogen protonated, and each pyridine oxygen deprotonated. It is interesting to note that **2**s form a polymer structure in the crystal by C(4′)–c(14′) covalent-bond formation, two Cu(II)–O(3P) and o(3p) coordinations, and two N(1)H···o(13p)

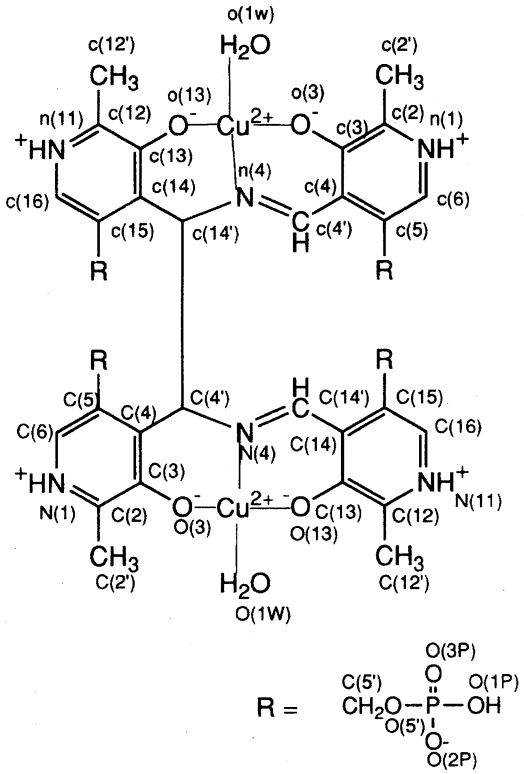

Fig. 1. Chemical structure of **2**, together with the atomic numbering used in this work. The thin lines represent coordination bonds. The numbering for phosphate group is presented only for C(5′), O(5), P(1), O(1P), O(2P), and O(3P) atoms. Same numbering system is cited for the remaining phosphate groups.

and n(1)H···O(13P) hydrogen bonds (Fig. 2 and Tables 2 and 3); this is a reason for the sparing solubility of the present crystals in aqueous solution. The copper ion forms an approximately square-pyramidal coordination with N(4), O(3), O(13), and O(1W) atoms in-plane and with an O(3P) atom translated by one unit cell in an apical position (Table 2). It is characteristic that the respective conformations of molecular fragments labeled with large and small letters are nearly C_2-symmetric related.

Thermal Stability of the Complex Structure. In order to investigate the structural stability of the complex, the thermal behavior was measured by a TG/DSC measurement.[10] There was no exothermic change accompanying the structural decomposition in the range of 20—130 °C, and no endothermic peak accompanied by melting was also observed within the temperature range. Two endothermic peaks were observed: $T_{max} = 95$ °C, $-\Delta H = 18.4$ kJ mol^{-1} for peak A and $T_{max} = 118$ °C, $-\Delta H = 155.2$ kJ mol^{-1} for peak B. The weight loss in the TG curve corresponds to the release for 1 water molecule of crystallization for peak A and 4 water molecules for B per dimer structure, respectively. Judging from the temperature factors for the respective water molecules in the crystal structure and their interactions with Schiff bases and/or copper ions, the O(1W) and o(1w) molecules, the thermal motions of which are relatively small, would be at least related to the $-\Delta H$ value of peak B, although it is difficult to assign the water molecules responsible for peak A. It is interesting to note that the same TG/DSC profile and $-\Delta H$ values are repeatedly obtained, when the complex crystal, which is recooled to 20 °C after heating to $\geq$130 °C, is again used for the measurement. This clearly indicates that the complex structure itself, including the coordination to copper ion, is thermally very stable.

Stereoselective Covalent Bond Formation. The lower dimer **2** (bold ellipsoid) in Fig. 2 corresponds to the (*R*,*R*)-configuration around the C(4′) and c(14′) atoms, and is linked through two Cu(II)–O(3P) coordination bonds with the upper **2** (fine ellipsoid) with the same (*R*,*R*)-configuration. Because of the centrosymmetric space group, a dimer with the (*S*,*S*)-configuration also exists in this crystal.

When the intermolecular C(4′) and c(14′) atoms are covalently linked between two neighboring Cu(II)·(PLP–PMP Schiff base) monomers (**1**), theoretically, four kinds of stereo-

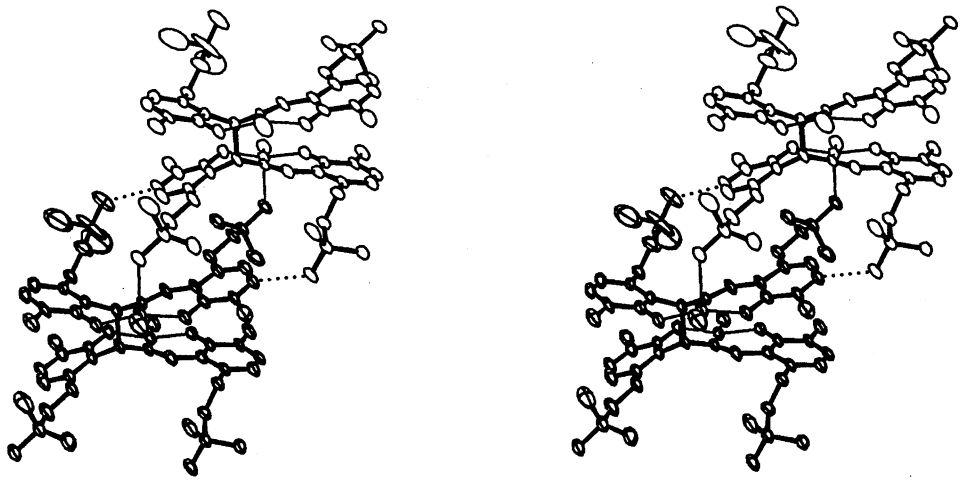

Fig. 2. Stereoscopic view of molecular conformation of **2** (bold ellipsoid) and its interaction with the adjacent **2** (fine ellipsoid) translated by one unit cell to *c*-direction. Both complexes are linked by two Cu(II)–O(3P) coordination bonds (thin lines) and two NH(pyridine)···O(phosphate) hydrogen bonds (dotted lines). The thermal ellipsoids of complexes are drawn at the 50% probability.

Table 1. Selected Structural Parameters

Bond lengths[a]			
N(1)–C(2)/n(11)–c(12)	1.34(2) Å		1.34(2) Å
N(1)–C(6)/n(11)–c(16)	1.33(2)		1.35(2)
N(11)–C(12)/n(1)–c(2)	1.33(2)		1.32(2)
N(11)–C(16)/n(1)–c(6)	1.32(2)		1.35(2)
P(1)–O(1P)/p(11)–o(11p)	1.56(1)		1.54(3)
P(1)–O(2P)/p(11)–o(12p)	1.48(1)		1.48(2)
P(1)–O(3P)/p(11)–o(13p)	1.488(9)		1.45(2)
P(11)–O(11P)/p(1)–o(1p)	1.555(9)		1.55(1)
P(11)–O(12P)/p(1)–o(2p)	1.52(1)		1.48(1)
P(11)–O(13P)/p(1)–o(3p)	1.477(9)		1.492(9)
C(3)–O(3)/c(13)–o(13)	1.32(1)		1.30(1)
C(13)–O(13)/c(3)–o(3)	1.30(1)		1.29(1)
C(4)–C(4′)/c(14)–c(14′)	1.51(2)		1.53(2)
C(4′)–N(4)/c(14′)–n(4)	1.48(1)		1.46(2)
N(4)–C(14′)/n(4)–c(4′)	1.30(2)		1.30(2)
C(14′)–C(14)/c(4′)–c(4)	1.48(2)		1.46(2)
C(4′)–c(14′)		1.62(2)	
Bond angles[a]			
C(2)–N(1)–C(6)/c(12)–n(11)–c(16)	124.7(9)°		124.6(8)°
C(12)–N(11)–C(16)/c(2)–n(1)–c(6)	124.7(8)		124.6(8)
C(4)–C(4′)–N(4)/c(14)–c(14′)–n(4)	113.2(6)		112.8(6)
C(14)–C(14′)–N(4)/c(4)–c(4′)–n(4)	122.7(7)		124.7(7)
C(4′)–N(4)–C(14′)/c(14′)–n(4)–c(4′)	113.1(7)		115.2(8)
c(14′)–C(4′)–C(4)		110.8(7)°	
c(14′)–C(4′)–N(4)		104.9(6)	
C(4′)–c(14′)–c(14)		112.1(7)	
C(4′)–c(14′)–n(4)		105.9(6)	
Torsion angles[a]			
C(4)–C(4′)–N(4)–C(14′)/c(14)–c(14′)–n(4)–c(4′)	−141(1)°		−138(1)°
C(4′)–N(4)–C(14′)–C(14)/c(14′)–n(4)–c(4′)–c(4)	−168(1)		−168(1)
C(4)–C(4′)–c(14′)–c(14)		49(1)°	
C(4)–C(4′)–c(14′)–n(4)		173(1)	
N(4)–C(4′)–c(14′)–c(14)		172(1)	
N(4)–C(4′)–c(14′)–n(4)		−65.0(9)	
Shift of N(4) atom from the plane I[b] or II[c]			
I	0.87(2) Å		0.88(2) Å
II	0.13(2)		0.14(2)

a) The values of the first and second columns correspond to the atomic combinations of the left and right sides, respectively. b) Left and right values are calculated from the planes of (N(1), C(2), C(3), C(4), C(5), C(6), C(4′)) and of (n(11), c(12), c(13), c(14), c(15), c(16), c(14′)), respectively. c) Left and right values are calculated from the planes of (N(11), C(12), C(13), C(14), C(15), C(16), C(14′)) and of (n(1), c(2), c(3), c(4), c(5), c(6), c(4′)), respectively.

isomers are possible for dimer formation, i.e., the (*R*,*R*), (*S*,*S*), (*R*,*S*), and (*S*,*R*) configurations at the (C(4′), c(14′)) position. Among them, the present dimer (**2**), consisting of the former two isomers, could be formed by the covalent-bond formation of two antiparallel-stacked **1**s, as schematically shown in Fig. 3(a). In fact, the preliminary crystal structure[12] of **1** showed such an intermediate state for dimer formation (see the left side of Fig. 3(a)), which was stabilized by two C(4′)···c(14′) and C(14′)···c(4′) short contacts of 2.3 Å, together with two intermolecular phosphate O–Cu(II) coordinations; the detailed crystal analysis will be reported in a forthcoming paper. On the other hand, as could be supposed from Fig. 3(b), the formation of the (*R*,*S*) or (*S*,*R*) isomer appears to be unfavorable, compared with the formation of the (*R*,*R*) or (*S*,*S*) isomer, because an intermediate state for such dimer formation would be energetically disadvantageous. In this meaning, the dimer formation of **2** could be stereoselective.

Crystal Structure. The crystal packing of **2** complexes and interactions with water molecules are schematically shown in Fig. 4. Possible hydrogen bonds are summarized in Table 3.

It is characteristic that layers consisting of the respective **2**s and water molecules are alternatively arranged perpendicular to the *b*-axis; this is a reason why the present crystals are very liable to easily crack perpendicular to this axis. As is obvious from Fig. 4, it appears interesting to note that a pseudo center of symmetry could be observed between the locations

Table 2. Coordination Parameters around Copper Ion[a,b]

Cu–O(3)/cu–o(13)	1.907(9) Å	1.909(9) Å
Cu–N(4)/cu–n(4)	1.964(9)	1.967(9)
Cu–O(13)/cu–o(3)	1.903(8)	1.900(9)
Cu–O(1W)/cu–o(1w)	1.99(1)	1.97(1)
Cu–o(3p)/cu–O(3P)	2.339(8)	2.485(9)
O(3)–Cu–N(4)/o(13)–cu–n(4)	93.1(4)°	93.2(4)°
O(3)–Cu–O(13)/o(13)–cu–o(3)	165.3(4)	163.2(4)
O(3)–Cu–O(1W)/o(13)–cu–o(1w)	87.3(4)	88.3(4)
O(3)–Cu–o(3P)/o(13)–cu–O(3P)	99.4(3)	101.7(3)
N(4)–Cu–O(13)/n(4)–cu–o(3)	91.8(4)	91.2(4)
N(4)–Cu–O(1W)/n(4)–cu–o(1w)	175.3(4)	176.7(4)
N(4)–Cu–o(3p)/n(4)–cu–O(3P)	91.1(3)	89.9(3)
O(13)–Cu–O(1W)/o(3)–cu–o(1w)	86.7(4)	88.2(4)
O(13)–Cu–o(3p)/o(3)–cu–O(3P)	94.3(3)	94.6(3)
O(1W)–Cu–o(3p)/o(1w)–cu–O(3P)	93.4(3)	86.8(4)

a) The values concerning Cu–o(3p) and cu–O(3P) atomic pairs were calculated for the combination of Cu (at x, y, z)–o(3p) (at x, y, z+1) and cu (at x, y, z)–O(3P) (at x, y, $z-1$), respectively. b) The values of the first and second columns correspond to the atomic combinations of the left and right sides, respectively.

of O(1W)~O(7W) and o(1w)~o(7w) water molecules, although these are crystallographically independent. The most significant deviation from the symmetry is observed between the O(6W) and o(6w) molecules. Consequently, the hydrogen bonds in which water molecules participate are slightly different from each other, although the water molecules are all located among **2** layers, and stabilize the crystal packing by participating in two to three hydrogen bonds with the polar atoms of neighboring **2**s and/or water molecules (Table 3).

One notable feature in the crystal structure is observed for the conformation of the phosphate groups (Table 4). While the remaining phosphate groups are all restricted in their motions, only the phosphate of p(11)~o(13p) endures the large thermal motion, in spite of their similar crystal environment (also see Fig. 2). A possible reason for this is because the oxygen atoms of p(11)~o(13p) participate in neither the coordination bonds nor the hydrogen bonds.

Formation Pathway of 2. It is interesting to note that a reaction solution of L-amino acid, such as alanine, leucine, lysine, glutamic acid, or glutamine, gave identical greenish **2**s through an in vitro chemical reaction. The time profile of the absorption spectral change[10] suggested the usual transamination progress of L-amino acid by PLP (**3**) according to the scheme shown in Fig. 5.[4] In the case of L-alanine, the absorption spectrum showing λ_{max} at ca. 400 nm, which is characteristic for the aldimine form (**4**) of PLP–amino acid Schiff base,[13] appeared at the initial stage of the reaction but decreased with the lapse of the reaction time, together with

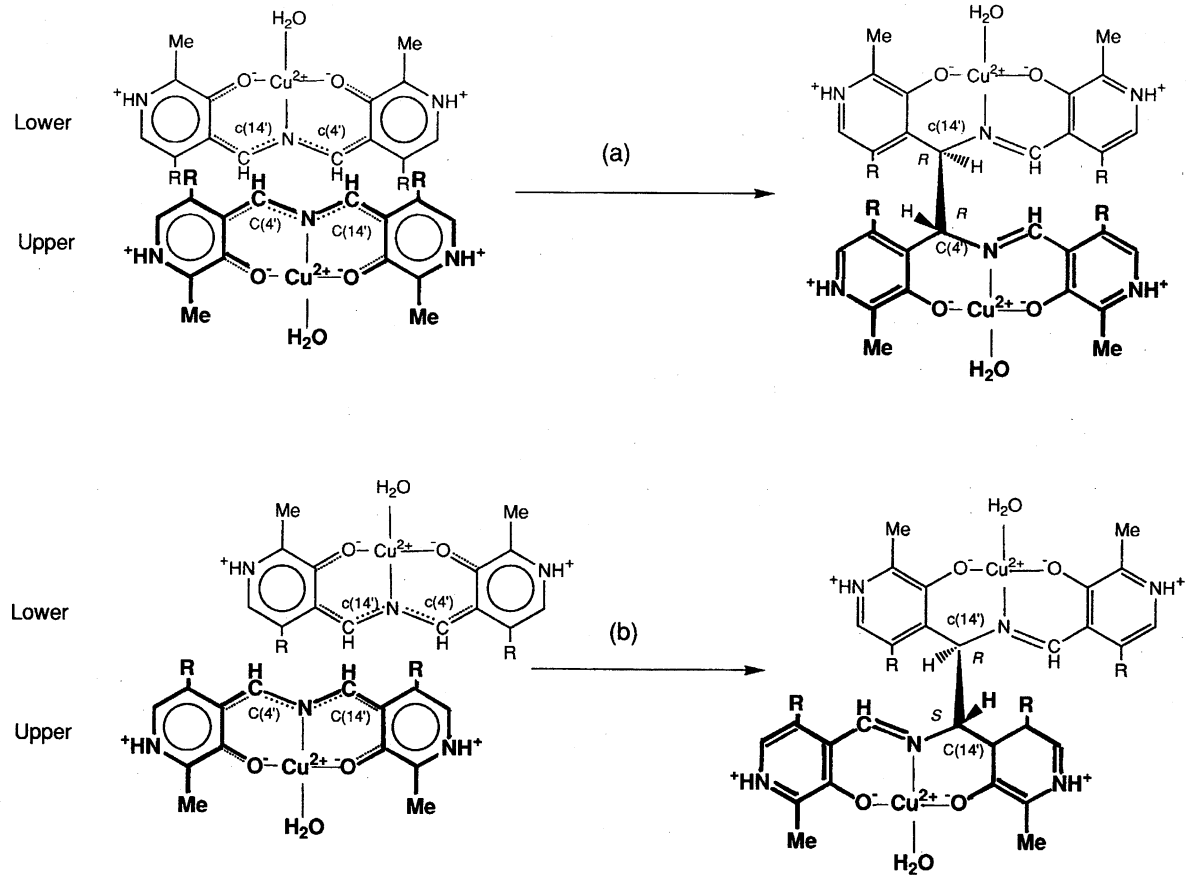

Fig. 3. Possible dimer formation with (*R*,*R*)- (a) or (*R*,*S*) stereoisomer from the two antiparallel-stacked **1** monomers by the σ-covalent bond formation at the intermolecular C(4′)···c(14′) or C(14′)···c(14′) atomic pair, respectively. Dimer of (*S*,*S*)- or (*S*,*R*) stereoisomer is formed by a covalent bond formation at C(14′)···c(4′) (a) or C(4′)···c(4′) (b) atomic pair, respectively.

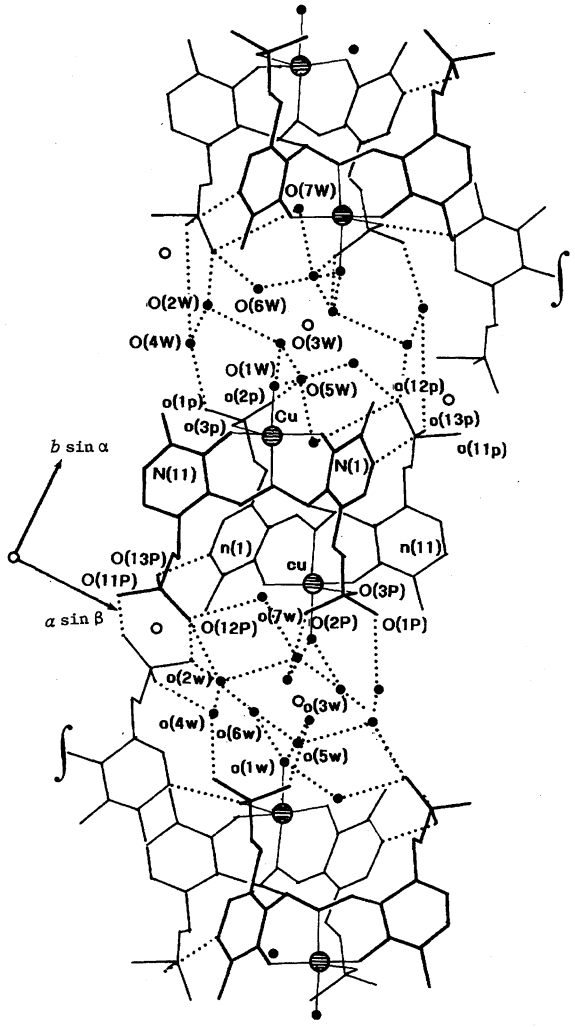

Fig. 4. Schematic view of crystal packing of **2**s and their interaction with water molecules in the crystal structure. Filled circles indicate water molecules, and dotted and thin lines represent possible hydrogen bonds and coordination bonds, respectively. Open circle stands for the crystallographic center of symmetry. The mark "$\int$" represent the repetition of the structure.

Table 3. Possible Hydrogen Bonds (< 3.0 Å)[a,b]

Donor	Acceptor	Distance (Å)	Distance (Å)
N(1)	O(13P)	2.53(2)^{I}	2.64(1)^{II}
N(11)	O(3P)	2.63(1)^{III}	2.61(1)^{IV}
O(11P)	O(12P)	2.55(1)^{V}	
O(1W)	O(6W)	2.80(2)^{VI}	2.66(3)^{VII}
O(2W)	O(12P)	2.87(3)^{VIII}	2.89(2)^{V}
O(2W)	O(3W)	2.71(2)^{VI}	
O(2W)	O(4W)	2.75(2)^{I}	2.88(2)^{II}
O(3W)	O(2P)	2.74(2)^{I}	2.73(2)^{II}
O(3W)	O(1W)	2.77(2)^{VI}	2.79(2)^{VI}
O(4W)	O(1P)	2.58(2)^{VI}	2.70(2)^{IX}
O(4W)	O(13P)	2.68(2)^{IX}	2.75(2)^{VI}
O(5W)	O(2P)	2.63(4)^{VI}	2.76(2)^{VI}
O(5W)	O(2W)		2.98(3)^{V}
O(5W)	O(3W)	2.72(4)^{VIII}	
O(5W)	O(6W)		2.62(3)^{VII}
O(6W)	O(11P)		2.91(3)^{VI}
O(6W)	O(12P)	2.65(3)^{VI}	
O(7W)	O(12P)	2.51(3)^{VI}	2.94(2)^{VI}
O(7W)	O(5W)	2.40(5)^{VI}	2.79(3)^{VI}

a) Hydrogen bonds correspond to the distances (Å) between the donor atom at x, y, z and the acceptor atom translated by the symmetry operation marked with the suffix superscript of I: x, y, z+1; II: x, y, $z-1$; III: $x-1$, y, $z-1$; IV: x+1, y, z+1; V: $1-x$, $-y$, $1-z$; VI: x, y, z; VII: x+1, y, z; VIII: $1-x$, $1-y$, $1-z$; IX: $x-1$, y, z. b) The first column corresponds to the distance between the donor atom of large letter and the acceptor atom of large or small one, and the second column to the distance between the donor atom of small letter and the acceptor atom of large or small one, respectively.

an increase in the absorbance at ca. 360 nm. By a comparison with an authentic synthetic or commercial sample, the conversion of the PLP–alanine Schiff base to PMP–copper-(II) complex (**7**) was indicated; the production of pyruvic acid (α-keto acid of the starting L-alanine) was ascertained by a method of Tatsumoto et al.[14] Since no spectral change was observed in the reaction solution without $Cu(NO_3)_2$, this reaction could be metal ion-dependent. As already discussed in the preceding paragraph (see Fig. 3), **2** could be formed via complex **1**. Since **2** underwent no further metabolic reaction

Table 4. Conformational Comparison around Phosphate Groups[a]

C(4)–C(5)–C(5′)–O(5)/c(14)–c(15)–c(15′)–o(15)	−171(1)	−81(1)
C(6)–C(5)–C(5′)–O(5)/c(16)–c(15)–c(15′)–o(15)	13(1)	97(1)
C(5)–C(5′)–O(5)–P(1)/c(15)–c(15′)–o(15)–p(11)	−173(1)	−173(1)
C(5′)–O(5)–P(1)–O(1P)/c(15′)–o(15)–p(11)–o(11p)	72.5(8)	73(1)
C(5′)–O(5)–P(1)–O(2P)/c(15′)–o(15)–p(11)–o(12p)	−48.2(8)	−54(1)
C(5′)–O(5)–P(1)–O(3P)/c(15′)–o(15)–p(11)–o(13p)	−173.6(8)	−180(1)
C(14)–C(15)–C(15′)–O(15)/c(4)–c(5)–c(5′)–o(5)	74(1)	163(1)
C(16)–C(15)–C(15′)–O(15)/c(6)–c(5)–c(5′)–o(5)	−103(1)	−15(1)
C(15)–C(15′)–O(15)–P(11)/c(5)–c(5′)–o(5)–p(1)	158(1)	150(1)
C(15′)–O(15)–P(11)–O(11P)/c(5′)–o(5)–p(1)–o(1p)	−60.5(7)	−67.8(8)
C(15′)–O(15)–P(11)–O(12P)/c(5′)–o(5)–p(1)–o(2p)	56.8(7)	51.4(8)
C(15′)–O(15)–P(11)–O(13P)/c(5′)–o(5)–p(1)–o(3p)	−178.1(7)	178.4(8)

a) The values of the first and second columns correspond to the atomic combinations of the left and right sides, respectively.

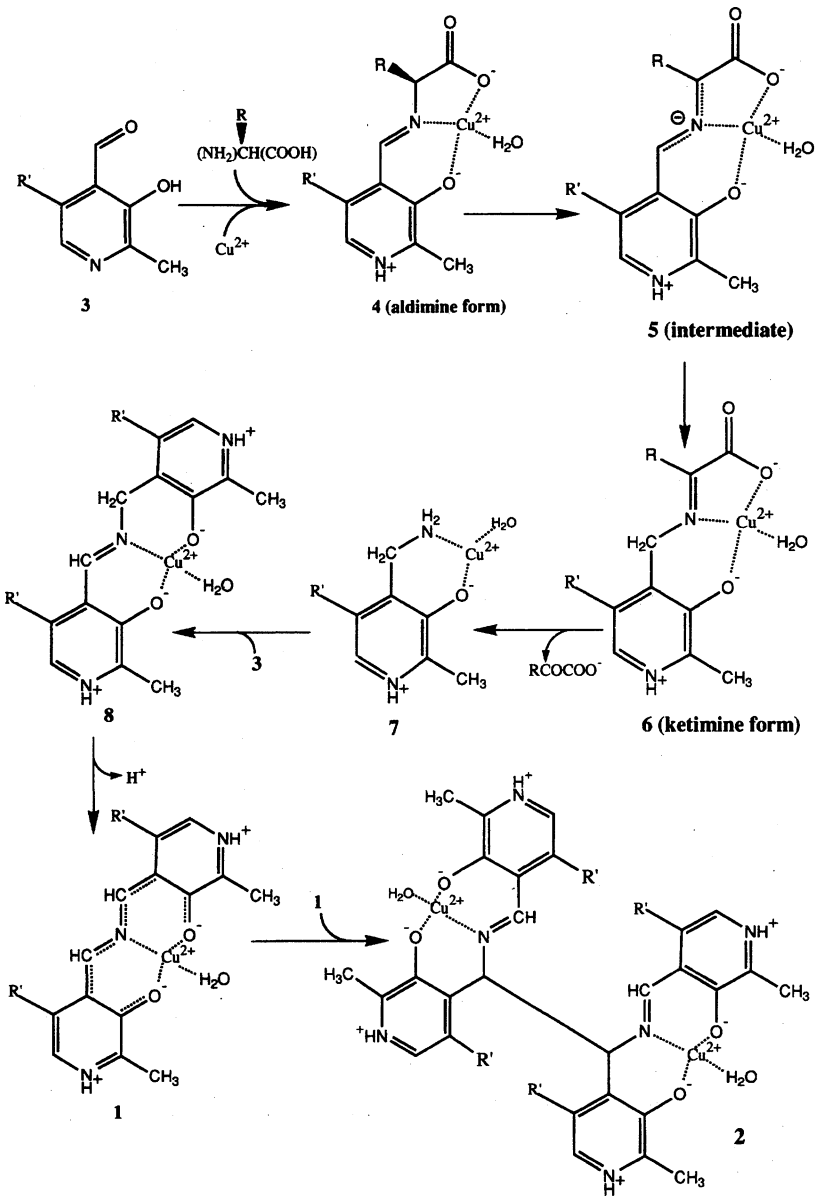

Fig. 5. Possible pathway for the copper(II)-mediated **2** production from PLP and L-amino acid in vitro.

throughout the experiment during about two months, it could be an end product.

Experimental

Materials. All starting materials of special grade were purchased from commercial companies. Spectroscopic-grade solvents and deionized water were used for all spectroscopic measurements and crystallization. The syntheses of PLP–PMP, pyridoxal (PL)–pyridoxamine (PM) and PLP–amino acid Schiff bases were carried out according to the literature.[15,16]

Preparation of Complex Crystals. To an aqueous solution containing equimolar PLP and $Cu(NO_3)_2$ (10 mM), an excess of L-alanine (15 mM) was added and adjusted to pH = 2.5 by HNO_3 or NaOH. In order to monitor the in vitro Cu(II)-mediated transamination reaction, the solution was kept at 20 °C for over two months, where the concentration was kept constant. Greenish platelet crystals (**2s**) were precipitated from the reaction solution within 1—2 weeks. Identical complexes were also obtained from L-amino acid of leucine, lysine, glutamic acid, or glutamine, instead of alanine.

Spectral Measurements. The UV/visible spectral change of the reaction solution was monitored as a function of the reaction time and of the pH using the JASCO UVIDEC 610A spectrometer. The molar absorption coefficients (ε) of the complex at respective λ_{max} are as follows: $\varepsilon_{294\ nm} = 10080$ and $\varepsilon_{329\ nm} = 3269$ for pH = 2.5; $\varepsilon_{295\ nm} = 7023$, $\varepsilon_{324\ nm} = 4023$ and $\varepsilon_{388\ nm} = 3562$ for pH = 3.0; $\varepsilon_{321\ nm} = 4694$ and $\varepsilon_{387\ nm} = 5972$ for pH = 7.0; $\varepsilon_{268\ nm} = 7062$ and $\varepsilon_{389\ nm} = 6559$ for pH = 11.0.

Thermal Analysis. The gravimetric and calorimetric changes (ΔW and ΔH) accompanying the heating of the complex crystals were monitored by thermogravimetry (TG) and differential scanning calorimetry (DSC) instruments, respectively (Rigaku, Japan). Al_2O_3 was used as a standard compound. The temperature from 10 to 130 °C was monitored, where the heating rate was set to 0.5 °C min^{-1}. Crystals of **2s** were dried in a desiccator for 24 h (total weight of 1.5—4.5 mg) and loaded into aluminum cells.

X-Ray Crystal Structure Determination. A single crystal having dimensions of 0.3×0.2×0.1 mm was sealed in a glass

capillary containing some mother liquid to prevent the release of water molecules of crystallization, and was used for X-ray diffraction studies on a Rigaku AFC-5 diffractometer employing graphite-monochromated Cu $K\alpha$ radiation. A summary of the crystallographic data at 15 °C is given in Table 5. The unit-cell dimensions were determined by a least-squares fit of 2θ angles for 18 reflections of $20° \leq 2\theta \leq 40°$. The crystal density was measured by the flotation method using a CCl_4–C_6H_6 mixture. Intensity data within $2\theta = 124°$ were collected with an ω–2θ scan mode, where the backgrounds were counted for 5s at both extremes of each reflection peak. The weak X-ray intensities [$F_o^2 < \sigma(F_o^2)$] were rescanned several times (up to 7 scans) to ensure good counting statistics. Four standard reflections were monitored for every 100 reflection intervals throughout the data collection, showing a random variation of $< \pm 1\%$ without significant trends. The observed intensities were corrected for the Lorentz and polarization effects. An empirical absorption correction was also applied.[17]

The complex structure was solved by the heavy atom method, and water molecules of crystallization were located by successive Fourier syntheses. The positional parameters of non-H atoms were refined by a full-matrix least-squares method with isotropic thermal parameters, and then with anisotropic thermal parameters (SHELXL-93 program[18]). The geometrically ideal positions of the H atoms were calculated and included in the calculation of the structure factors. The function of $\Sigma w(F_o^2 - F_c^2)^2$ was minimized and $w = [\sigma(F_o^2)^2 + (0.1376p)^2 + 16.58p]^{-1}$ was used, where $p = (\mathrm{Max}(F_o^2, 0) + 2F_c^2)/3$. The final $R1$ [$\Sigma||F_o| - |F_c||/\Sigma|F_o|$], $wR2$ [$(\Sigma w(F_o^2 - F_c^2)^2/\Sigma w(F_o^2)^2)^{1/2}$], and S[$(\Sigma w(F_o^2 - F_c^2)^2/(M-N))^{1/2}$, where M = no. of reflections with $F_o^2 > 2\sigma(F_o^2)$ and N = no. of variables used for the refinement] are also given in Table 5. None of the positional parameters of the non-H atoms shifted by more than one-third from their estimated standard deviations, and the unassigned electron density in the final stage of the refinement was in the range of -1.280 to 1.860 eÅ^{-3} around the copper ions. The atomic scattering factors and terms of anomalous dispersion corrections were taken from the usual source.[19] All numerical calculations were carried out at the Computer Center, Osaka University of Pharmaceutical Sciences.

Table 5. Summary of Crystal Data and Intensity Collection Details

Formula	$Cu(II)_2 \cdot C_{32}H_{36}N_6O_{20}P_4 \cdot 14H_2O$
MW	1327.86
Crystal system	Triclinic
Space group	$P\bar{1}$
a/Å	10.880(2)
b/Å	25.280(3)
c/Å	9.850(1)
α/°	95.89(1)
β/°	92.74(1)
γ/°	92.04(1)
V/Å^3	2689.4(6)
Z	2
D_m/g cm^{-3}	1.615(5)
D_x/g cm^{-3}	1.640
μ(Cu $K\alpha$)/mm^{-1}	3.03
$F(000)$	1376
T of data collection/°C	15
Scan speed in 2θ/°min^{-1}	4
Scan range in ω/°	$1.511 + 0.15 \tan\theta$
No. of unique data measured	8486
No. of data used for refinement	3835 [$F_o^2 > 2\sigma(F_o^2)$]
No. of variables	721
R_1	0.086
wR_2	0.336
S	1.145

References

1) D. M. Smith, N. R. Thomas, and D. Gani, *Experientia*, **47**, 1104 (1991).

2) D. Dolphin, R. Poulson, and O. Avramovic, "Vitamin B_6, Pyridoxal Phosphate, Chemical, Biochemical and Medical Aspects," John Wiley & Sons, New York (1986), Part B.

3) D. E. Metzler and E. E. Snell, *J. Biol. Chem.*, **198**, 353 (1952).

4) A. E. Martell, in "Advances in Enzymology," ed by A. Meister, John Wiley & Sons, New York (1982), Vol. 53, pp. 163—199.

5) L. Leussing, in "Vitamin B_6, Pyridoxal Phosphate, Chemical, Biochemical and Medical Aspects," ed by D. Dolphin, R. Poulson, and O. Avramovic, John Wiley & Sons, New York (1986), Part A, pp. 69—115.

6) H. C. Dunathan, *Adv. Enzymol. Relat. Area Mol. Biol.*, **35**, 79 (1971).

7) M. M. Palcic and H. G. Floss, in "Vitamin B_6, Pyridoxal Phosphate, Chemical, Biochemical and Medical Aspects," ed by D. Dolphin, R. Poulson, and O. Avramovic, John Wiley & Sons, New York (1986), Part A, pp. 25—68.

8) M. Darriet, M. J. Basurko, A. Cassaigne, and J. Darriet, in "Vitamin B_6, Pyridoxal Phosphate, Chemical, Biochemical and Medical Aspects," ed by D. Dolphin, R. Poulson, and O. Avramovic, John Wiley & Sons, New York (1986), Part A, pp. 265—307.

9) T. Ishida, K. Hatta, S. Yamashita, M. Doi, and M. Inoue, *Chem. Pharm. Bull.*, **34**, 3553 (1986).

10) Lists of atomic coordinates, anisotropic temperature factors of non-H atoms, bond lengths, bond angles, torsion angles, and observed and calculated structure factors, DSC profile of the complex as a function of temperature, and time-profile of absorption spectrum of reaction solution (pH = 2.5) of PLP, $Cu(NO_3)_2$, and L-alanine at 20 °C with aeration are deposited as Document No. 70038 at the Office of the Editor of Bull. Chem. Soc. Jpn.

11) F. H. Allen, O. Kennard, D. G. Watson, L. Brammer, A. G. Orpen, and R. Taylor, *J. Chem. Soc., Perkin Trans. 2*, **1987**, S1.

12) T. Ishida, Y. In, H. Nagata, M. Doi, and A. Wakahara, *Chem. Lett.*, **1995**, 1137.

13) A. E. Martell and V. M. Shanbhag, *J. Chem. Soc., Chem. Commun.*, **1990**, 352.

14) K. Tatsumoto, M. Haruta, and A. E. Martell, *Inorg. Chim. Acta*, **138**, 231 (1987).

15) M. Ikawa, *Arch. Biochem. Biophys.*, **118**, 497 (1967).

16) F. Nepveu, J.-J. Bonnet, and J.-P. Laurent, *J. Coord. Chem.*, **11**, 185 (1981).

17) A. C. T. North, D. C. Phillips, and F. S. Mathews, *Acta Crystallogr., Sect. A*, **A24**, 351 (1968).

18) G. M. Sheldrick, "SHELXL-93: A Program for the Refinement of Crystal Structures from Diffraction Data," University of Göttingen (1993).

19) "International Tables for X-Ray Crystallography," Kluwer Academic Publishers, Dordrecht (1992), Vol. C.